2008 IEEE International Conference on
Robotics and Automation
Pasadena, CA, USA, May 19-23, 2008

Simulated Regulator to Synthesize ZMP Manipulation and Foot Location for Autonomous Control of Biped Robots

Tomomichi Sugihara

Abstract— **An autonomous biped controller synthesizing the ZMP manipulation and the foot location is proposed; each of them has a strongly nonlinear property, so that they had been hard to be synthesized without referential trajectories given as functions of time. The former is equivalent to the partial indirect manipulation of the reaction force through the contact points with the environment to control the center of mass (COM) under the current supporting state. The latter means discontinuous relocation of grounding feet in order to deform the supporting region to include the desired but unachievable ZMP in the future. They run on an identical control system without any confliction, since they originate from the same simulated regulator in the sense that the feasible region of ZMP is not bounded. It is also shown that a cyclic walk is automatically generated without giving a walking period explicitly by coupling the support-state transition and the goal-state transition in a simulation.**

I. INTRODUCTION

Biped robots have potentially high mobilities. Since they have similar morphologies with the humans' lower limbs, they are expected to grow up into the robots which can travel wherever humans can. To make biped robots catch up with such an expectation still needs to resolve many challenges.

The two bases of pedipulation, namely, the legged motion control are the indirect reaction force manipulation [1][2] [3][4] and the discontinuous grounding foot location [5][6] [7][8]. The former is necessary to transport the center of mass (COM) of the floating multibody system, which is not mechanically connected to the inertial frame. The latter is required to reform the supporting region of the system, which determines the limitation of the physically available rection forces. Each has a strongly nonlinear property, so that the synthesis of them is still an open problem.

A major solution against it is to refer the motion trajectory which is defined as a function of time. It can coordinate the fullbody motion involving foot location and COM transportation rather easily with physical feasibility represented by ZMP[9] and geometric constraints such as collision avoidance taken into account. Many successful biped walkers based on this approach have been appeared [10] [11] [12] [13] [14] [15] [16] [17]. Such time-slaved controls, however, are not robust against various extrinsic events. While they work in situations where sufficient knowledge about the environment and the task is given in advance, they are less promising in the fields of action with many uncertainties which are hard to be modelled. It is desired that the control system is designed as an autonomous system, namely, a system which does not explicitly depend on time.

Mitobe et al.[3], Fujimoto et al.[4] and the authors[18] also proposed COM control methods by manipulating the reaction force or ZMP in realtime. They focused on the COM control under a given supporting condition, and the foot location strategies were out of the scope. Gubina et al.[19], Kajita et al.[20] and Westervelt et al.[21] proposed autonomous biped controllers. They are stepwise-stable in accordance with the point-foot contact. The application to the realistic robots which support themselves on their sole has been a future work. Passive dynamic walking [22] [23] [24] is another approach to design an autonomous biped controller by utilizing an inherent stability of discretized biped dynamics. It stands on the ideally perfect plastic collision between the robot and the ground, and thus, has a low stabilizing ability.

This paper proposes a control to synthesize the above the ZMP manipulation control and the foot location with a consistency. We design a regulator based on the approximate dynamical model of a biped robot, focusing on a simple relationship between COM and ZMP. In this stage, the feasible area where ZMP can exist is unbounded against the physical constraint. In this sense, we call it the simulated regulator. When the desired ZMP is located out of the supporting region, it is modified to be consistent with the actual region. The robot is controlled in such a way that the real ZMP tracks the desired ZMP. Simultaneously, the supporting region is deformed by a foot replacements to include the original desired ZMP and to resolve the inconsistency which would happen in the future. The regulator gains are decided by the pole assignment method in order to give COM a slow mode and ZMP a fast mode explicitly, which matches the role of each foot. Since both the ZMP manipulation and the foot location originate from the identical simulated regulator, a totally consistent control system is made up. In addition, it is shown that a cyclic walk is automatically generated without giving a walking period explicitly by coupling the support-state transition and the goal-state transition. It does not assume a periodicity of the motion trajectory, and hence, seamless starting and stopping can be achieved.

II. SIMULATED COM–ZMP REGULATOR

A. Linearized biped system and simulated regulator

The strict equation of motion of a biped robot takes a complicated form with tens of degrees-of-freedom. Here, we

This work was supported by "The Kyushu University Research Superstar Program (SSP)", based on the budget of Kyushu University allocated under President's initiative.

T. Sugihara is with School of Information Science and Electrical Engineering, Kyushu University, 744 Moto'oka, Nishi-ku, Fukuoka, Japan zhidao@ieee.org

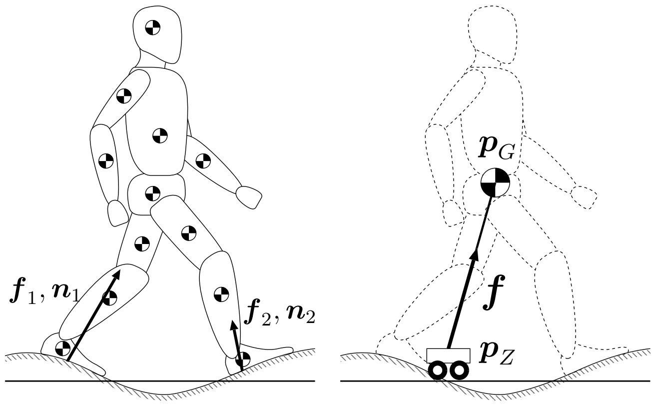

(a)Precise anthropomorphic model (b)Inverted pendulum metaphorized model

Fig. 1. Approximately mass-concentrated biped model.

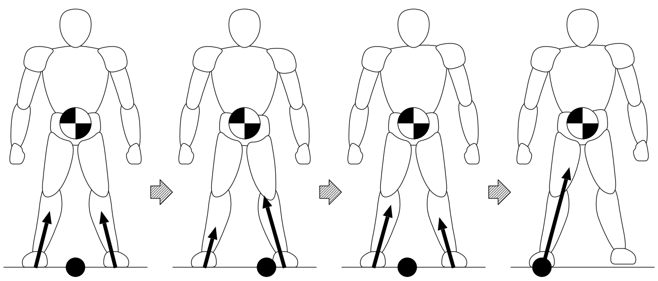

Fig. 2. Coupled movement of ZMP and COM in the ground-kick in the double support phase. ZMP travels fast between the feet to overtake COM.

assume that an effect of the moment about COM is smaller enough to be neglected than that about ZMP due to the movement of COM. Then, the macroscopic behavior of the legged system is represented by the motion of COM. The equation of motion in horizontal direction of a biped model with such a mass-concentrated approximation as **Fig. 1**(B) is expressed as follows:

$$\ddot{x} = \omega^2(x - x_Z) \tag{1}$$

$$\ddot{y} = \omega^2(y - y_Z), \tag{2}$$

where $\boldsymbol{p}_G = [\, x \;\; y \;\; z \,]^{\mathrm{T}}$ is the position of COM, and $\boldsymbol{p}_Z = [\, x_Z \;\; y_Z \;\; z_Z \,]^{\mathrm{T}}$ is ZMP. ω is defined as:

$$\omega^2 \equiv \frac{\ddot{z} + g}{z - z_Z} \; \left(\geq 0 \right), \tag{3}$$

where g is the acceleration of gravity, and z_Z is the ground level, which is known. z, x and y axes are aligned along the gravity, the forward and the leftward directions, respectively. Eq.(1) and (2) imply that COM can be controlled via manipulation of ZMP.

The coupled movement of ZMP and COM is not simple. Let us consider a case where the robot lifts up one foot from the both-standing state, for example. Note that, in such situations, a conventional distinction between swing foot and stance foot is no longer meaningless, since neither feet are swinging. However, they are obviously different from each other in terms of function. In this paper, the foot to be the swing foot is called *kicking foot*, and that to be the stance foot is called *pivoting foot*, instead.

ZMP is required to be within the pivoting sole at the end of the phase in order to detach the kicking foot off the ground, while it moves into the sole of kicking foot in the initial phase in order to accelerate COM towards the pivoting foot. Namely, ZMP initially moves oppositly against the desired COM movement direction, and overtakes COM during the motion. The fact that the biped robot is a non-minimum-phase-transition system as well as the inverted pendulum underlies the requirement of such a complex manipulation of ZMP. In addition, ZMP travels faster than COM between the feet in the double support phase, as ZMP depends on the acceleration of the robot. Both modes of COM and ZMP movement are desired to be explicitly designed in accordance with the locations of feet. Then, we include ZMP in the state variable and regard the ZMP rate as the input. The linearized state equation is represented as follows:

$$\dot{\boldsymbol{x}} = \boldsymbol{A}\boldsymbol{x} + \boldsymbol{b}u, \tag{4}$$

where the motion along x-axis is only considered from the isomorphism of Eq.(1) and (2), and:

$$\boldsymbol{x} \equiv \begin{bmatrix} x \\ \dot{x} \\ x_Z \end{bmatrix}, \; \boldsymbol{A} \equiv \begin{bmatrix} 0 & 1 & 0 \\ \omega^2 & 0 & -\omega^2 \\ 0 & 0 & 0 \end{bmatrix}, \; \boldsymbol{b} \equiv \begin{bmatrix} 0 \\ 0 \\ 1 \end{bmatrix}, u \equiv \dot{x}_Z,$$

respectively. In the above equation assumed that the vertical movement of COM is slower enough to regard as $\omega \simeq \mathrm{const.}$ than the horizontal movement. The ZMP rate is decided based on the state feedback around the referential state ${}^{ref}\boldsymbol{x}$.

$$u = \boldsymbol{k}^{\mathrm{T}}({}^{ref}\boldsymbol{x} - \boldsymbol{x}). \tag{5}$$

The gain $\boldsymbol{k}$ is designed by the pole assignment method so as to embed a faster mode explicitly into ZMP movement than the mode of COM. The motion along y-axis is dealt with as well. In this stage, we don't constrain ZMP in the supporting region, so that the system is not necessarily physically consistent. In this sense, let us call it *the simulated ZMP* and represent it by $\tilde{\boldsymbol{p}}_Z = [\, \tilde{x}_Z \;\; \tilde{y}_Z \;\; z_Z \,]^{\mathrm{T}}$. As long as $\tilde{\boldsymbol{p}}_Z$ is within the supporting region, the actual desired ZMP ${}^{d}\boldsymbol{p}_Z$ is set for the same position with $\tilde{\boldsymbol{p}}_Z$.

Fig. 4 illustrates the idea of the proposed control. The situation where $\tilde{\boldsymbol{p}}_Z$ lies out of the supporting region means that COM cannot be provided with the desired acceleration under the current supporting condition. In order to compromise this inconsistency between the desired control and the actually executable control, the following two maneuvers are required. One is to take a physically-feasible acceleration which is the nearest to the desired value by setting the desired ZMP ${}^{d}\boldsymbol{p}_Z$ for the proximity of $\tilde{\boldsymbol{p}}_Z$ to the supporting region as **Fig. 3** depicts. The motion continuity at the moment of landing is held by resetting the simulated ZMP $\tilde{\boldsymbol{p}}_Z$ for the actually desired ZMP ${}^{d}\boldsymbol{p}_Z$. This idea has been already proposed by the authors [18]. The other is to deform and expand the supporting region so as to include $\tilde{\boldsymbol{p}}_Z$ in the future, which is described in the following section.

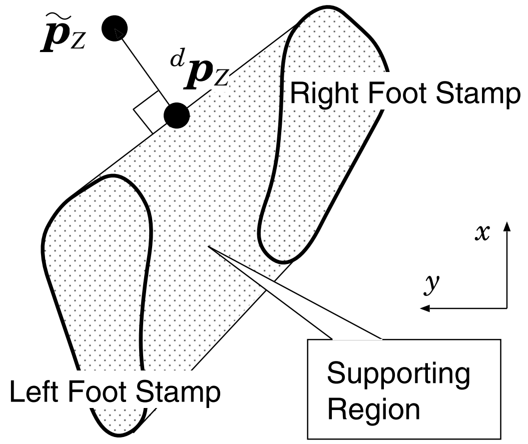

Fig. 3. Substitution of $\tilde{\boldsymbol{p}}_Z$ for ${}^d\boldsymbol{p}_Z$ to match the actual supporting region.

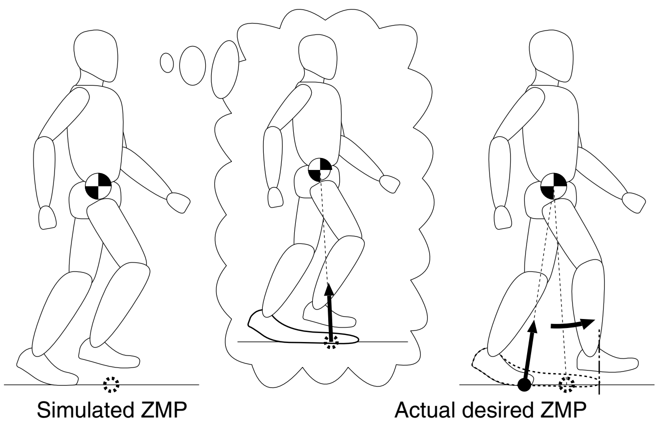

Fig. 4. The concept of the simulated regulator. When the simulated ZMP $\tilde{\boldsymbol{p}}_Z$ lies out of the supporting region, the desired ZMP ${}^d\boldsymbol{p}_Z$ is set for the proximity to the supporting region. At the same time, the swing foot is relocated to deform the supporting region so as to include $\tilde{\boldsymbol{p}}_Z$ in the future.

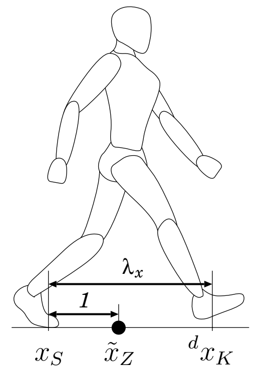

Fig. 5. Step ratio λ_x to cover simulated ZMP in the future.

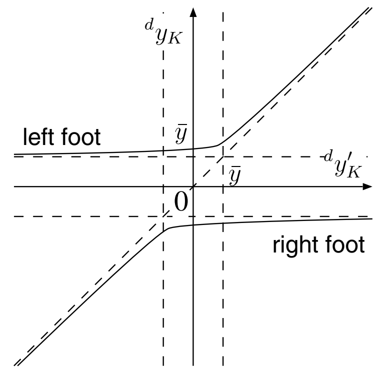

Fig. 6. Foot location transformation in y-axis for self-collision avoidance.

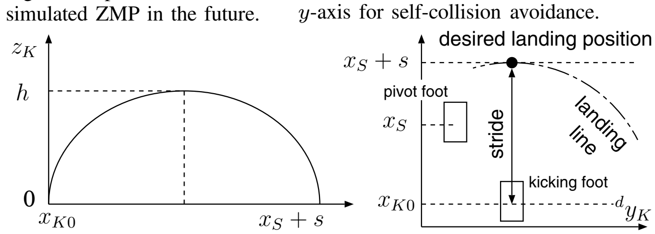

Fig. 7. Spatial foot trajectory (left) in xz-plane (right) in xy-plane.

B. Foot location control based on simulated ZMP

The deformation of the supporting region is achieved via the relocation of stance feet. Suppose ZMP is within the pivoting sole. Let us define that $\boldsymbol{p}_S = [\, x_S \;\; y_S \;\; z_S \,]^{\mathrm{T}}$ and $\boldsymbol{p}_K = [\, x_K \;\; y_K \;\; z_K \,]^{\mathrm{T}}$ are the tip positions of the pivoting foot and the kicking foot, respectively. They correspond to the positions of the stance foot and the swing foot during the single support phase, respectively. We decide the desired position of the foot ${}^d\boldsymbol{p}_K = [\, {}^dx_K \;\; {}^dy_K \;\; {}^dz_K \,]^{\mathrm{T}}$ by the following procedure.

The COM acceleration which the simulated regulator requires (called *the simulated COM acceleration*, hereafter), and the desired COM acceleration which conforms to the actual supporting condition (called *the desired COM acceleration* in short, hereafter) are defined by the relative COM locations with respect to the simulated ZMP $\tilde{\boldsymbol{p}}_Z$ and the actually desired ZMP ${}^d\boldsymbol{p}_Z$, respectively. The necessity of a relocation of grounding feet, arises in case where the desired COM acceleration is inconsistent with the simulated COM acceleration. It is judged with respect to x- and y-axes independently. ${}^dx_K$ is defined as follows:

$$ {}^dx_K = \begin{cases} \lambda_x \tilde{x}_Z + (1-\lambda_x)x_S & (\text{for} \;\; \iota_x < 0) \\ x_K & (\text{for} \;\; \iota_x \geq 0) \end{cases} \tag{6} $$

$$ \iota_x \equiv (x - \tilde{x}_Z)(x - {}^dx_Z), \tag{7} $$

where λ_x is a constant to define the step magnitude ($\lambda_x > 1$). The above rule means that the robot puts its swing foot on the place where the desired COM acceleration orients to the same direction with the simulated COM acceleration, if they direct counterwards to each other.

For the motion in y-axis, ${}^dy'_K$ is firstly computed from the designed $\lambda_y (> 1)$ as well. Then, it is converted to ${}^dy_K$ by the following rule in order to avoid the self-collision between both leg:

$$ {}^dy_K = \bar{y} + \frac{1}{2}\left\{ {}^dy'_K - \bar{y} \pm \sqrt{({}^dy'_K - \bar{y})^2 + a} \right\}, \tag{8} $$

where $+$ is chosen for the left leg for the double sign, while $-$ for the right leg, and $\bar{y}$ is the inner boundary of the swing foot. The above function has a profile as **Fig. 6**. A smaller constant a makes the curve approach to the asymptotic lines with the break point $({}^dy'_K, {}^dy_K) = (\bar{y}, \bar{y})$.

Suppose the initial position of the swing foot is $\boldsymbol{p}_{K0} = [\, x_{K0} \;\; y_{K0} \;\; z_{K0} \,]^{\mathrm{T}}$, and the lift height of the swing foot ${}^dz_K$ is defined as:

$$ {}^dz_K = 2h\sqrt{\theta(1-\theta)} \tag{9} $$

$$ \theta \equiv \min\left\{ \frac{({}^dx_K - x_{K0})^2 + ({}^dy_K - y_{K0})^2}{|x_S - x_{K0} + s|}, 1 \right\}. \tag{10} $$

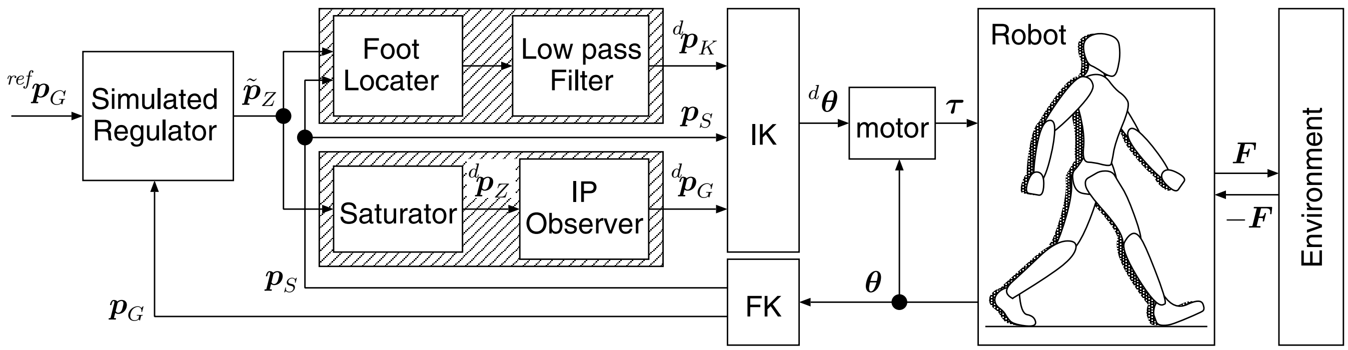

Fig. 8. Block diagram of the proposed biped control system with the simulated regulator.

It generates a spatial trajectory which carries the swing foot along a half ellipsoid with a height h as the leftside of **Fig. 7**, and makes it land on a circle with the center (x_{K0}, y_{K0}) and the radius $x_S - x_{K0+s}$, the bird's-eye view of which is depicted in the right side of **Fig. 7**; it lands to the point with a stride $x_S - x_{K0} + s$ from the initial position as long as ${}^{d}y_K = y_{K0}$ is ensured.

The above procedure does not guarantee the time continuity of ${}^{d}\boldsymbol{p}_K$, so that it might jump largly at the moment when ZMP travels to the pivoting sole, or when the relative COM location with respect to the simulated ZMP comes in the opposit side of that with respect to the desired ZMP, for instance. Then, the time sequence of ${}^{d}\boldsymbol{p}_K$ is smoothened by second-order low-pass filters, for example.

Fig. 8 is a block diagram of the proposed control system described above. 'IP Observer' in the figure shows a subsystem which outputs the desired COM position ${}^{d}\boldsymbol{p}_G$ equivalent to the desired ZMP ${}^{d}\boldsymbol{p}_Z$[18]. One can note that both the COM controller with ZMP manipulation and the foot relocation controller branch from the identical simulated regulator and join in the inverse kinematics solver (the motion rate resolver).

III. Autonomous walk by coupled goal-state/support-state transition

Suppose the referential COM position is ${}^{ref}\boldsymbol{p}_G = \begin{bmatrix} {}^{ref}x & {}^{ref}y & {}^{ref}z \end{bmatrix}^{\mathrm{T}}$, then, the referential state of the simulated regulator in x-axis is ${}^{ref}\boldsymbol{x} = \begin{bmatrix} {}^{ref}x & 0 & {}^{ref}x \end{bmatrix}^{\mathrm{T}}$. The control in the previous section yields a step motion automatically by locating ${}^{ref}\boldsymbol{p}_G$ out of the supporting region on purpose. This property is utilized to achieve an autonomous continual walk by coupling the referential goal state transition and the supporting state transition, namely, by repeating to set ${}^{ref}\boldsymbol{p}$ out of the supporting region after the supporting region is deformed so as to include ${}^{ref}\boldsymbol{p}_G$ by the stepping. More concretely, ${}^{ref}x$ is defined by the following equation for a given s and the position of pivoting foot x_S in x-axis:

$$ {}^{ref}x = x_S + rs, \tag{11} $$

where r is a certain positive coefficient ($0 < r < 1$). In cases where the robot changes the orientation, x- and y-axes are again realigned with respect to the moving direction, and the desired COM position is computed with the above Eq.(11).

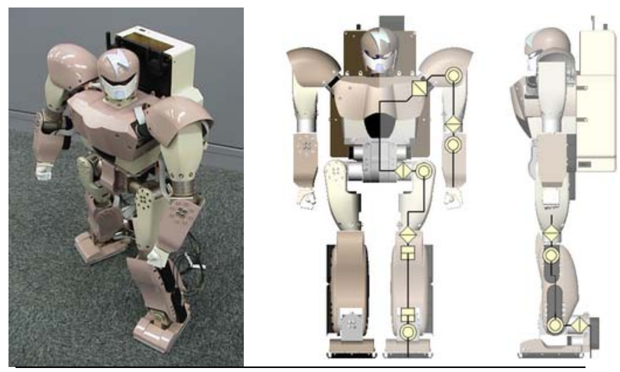

Height:	580 [mm]
Weight:	6.5 [kg]
Number of joints:	20 (8 for arms,12 for legs)

Fig. 9. External view and specifications of the robot "mighty".

IV. Simulation

We verified the proposed control via a simulation with an inverted pendulum model whose mass was concentrated at the tip. The length of the pendulum was 0.27[m], which fits to the robot "mighty"[25] shown in **Fig. 9**. Note that the robot mass does not affect the behavior of the inverted pendulum. The both sole were modelled as rectangles with the length 0.055[m] to the toe edge, 0.04[m] to the heel edge, and 0.035[m] to each side. The state feedback gains were designed by the pole assignment method. The poles were -3, -6 and -10 with respect to x-axis, and -2.5, -25 and -30 with respect to y-axis. The other control parameters were set for $\lambda_x = 2$, $\lambda_y = 3$, $a = 0.001$, $r = 0.9$ and $h = 0.01$[m], respectively. The desired swing foot position was smoothened by a second-order low-pass filter $\dfrac{1}{(0.02s+1)^2}$. The initial state was set for $(x, y) = (0, 0)$ and $(\dot{x}, \dot{y}) = (0, 0)$. The initial stance position of the left and the right feet were $(0, 0.045)$ and $(0, -0.045)$, respectively. From the first to the sixth step, the stride s was set for 0.3[m], and the referential COM position was automatically updated by the

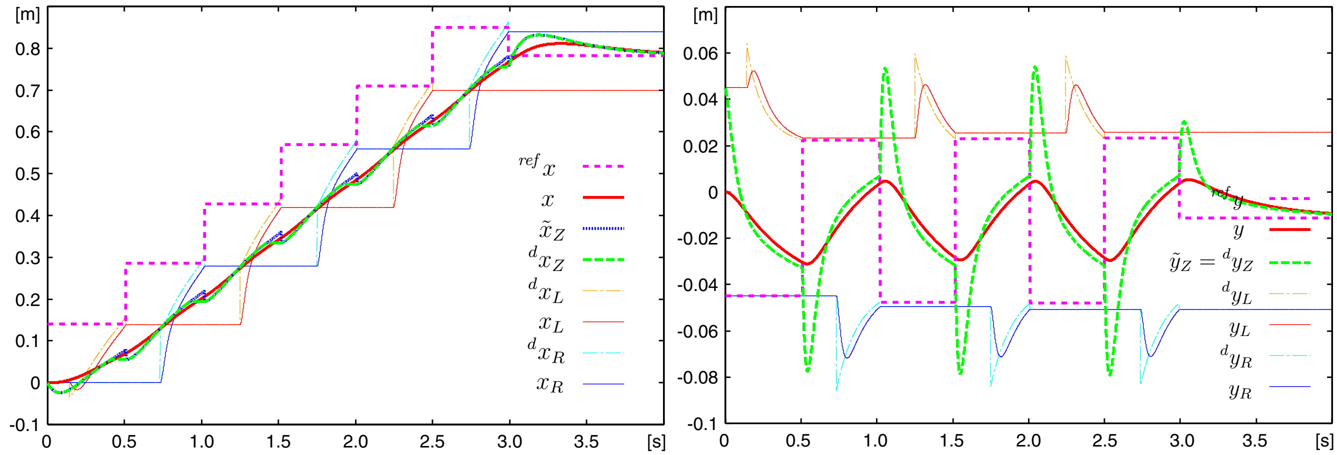

(a) Loci of COM, ZMP and feet in x-axis

(b) Loci of COM, ZMP and feet in y-axis

Fig. 10. Resulted loci of COM, ZMP and feet.

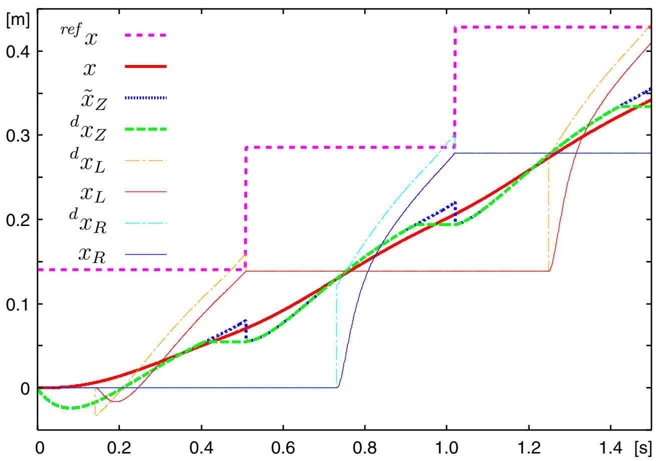

Fig. 11. Zoomed loci of COM, ZMP and feet.

method described in section III. Immediately after landing the sixth step, the referential COM position was settled at the midpoint of both feet.

The loci of the referential COM position $({}^{ref}x, {}^{ref}y)$, the actual COM (the tip point of the inverted pendulum)(x, y), the simulated ZMP position $(\tilde{x}_Z, \tilde{y}_Z)$, the actually desired ZMP position $({}^dx_Z, {}^dy_Z)$, the referential feet positions $({}^dx_L, {}^dy_L)$, $({}^dx_R, {}^dy_R)$ and the filtered positions of them (x_L, y_L), (x_R, y_R) are plotted in **Fig. 10**. It is seen that an almost cyclic continual walk was achieved without giving a walk period explicitly by an alternation of the supporting-region deformation via the pedipulation and the goal-state transition. In this example motion, the simulated ZMP and the actually desired ZMP in y-axis always coincided with each other, so that a sideward stepping was not resulted. The difference of COM and ZMP modes particularly appear in the movement along y-axis. The given pole to design feedback gains set the time-constant of the sideward kicking for about 0.1[s], which contributed to ensure about 60% of duty ratio of the swinging phase. **Fig. 11** zooms a part of **Fig. 10** from $t = 0 \sim 1.5$. ${}^dx_Z$ differs from $\tilde{x}_Z$ in $t \simeq 0.4 \sim 0.5$, $t \simeq 0.9 \sim 1.0$ and $t \simeq 1.4 \sim 1.5$. ${}^dx_Z$ in those terms are thought to be saturated at the toe edge of the supporting sole. $\tilde{x}_Z$ is synchronized at $t \simeq 0.5, 1.0$ when the swing foot lands on the ground, and the continuity of ZMP is held. ${}^dx_L$ and ${}^dx_R$ discontinuously jump at $t \simeq 0.15, 0.75, 1.25$ which are thought to be times when the ZMP reaches the pivoting sole. In spite of that, x_L and x_R keep continuous, thanks to the low-pass filters. The robot responded to the sudden stop of the reference at $t \simeq 3.0$ without bankruptcy. **Fig. 12** shows some sequential snapshots of a motion of the inverted pendulum. The red ball and the green ball in the figure indicate the referential COM position and the simulated ZMP position, respectively. The magenta area is the supporting region composed from the grounding sole. **Fig. 13** shows snapshots of the synthesized robot motion computed by the above result and the inverse kinematics. Note that the fullbody dynamics is not considered.

V. Conclusion

We developed an autonomous biped controller, in which the ZMP manipulation under the current support condition and the pedipulation to deform the future support region were synthesized. Both are based on an identical simulated regulator, so that they are integrated into the total control system without any confliction. Since the simulated regulator involves ZMP in the state variable, it is possible to give a slow mode to COM and a fast mode to ZMP, which is accommodated to the current choice of stance and kicking feet, explicitly by the pole assignment method.

The autonomous controller is promising to improve the system robustness against extrincic events and uncertainties in the environment. The next short-term issues are to verify the absorption performance of perturbations and to examine the adaptability against rough terrains.

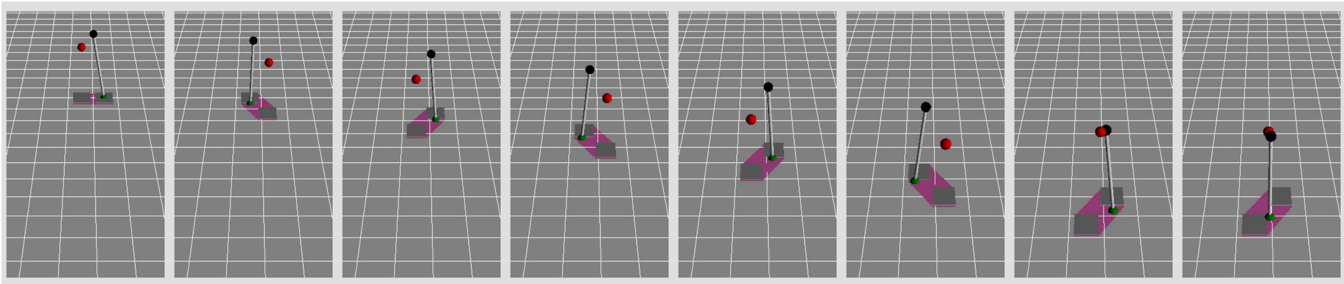

Fig. 12. Snapshots of an inverted pendulum motion controlled by the proposed method.

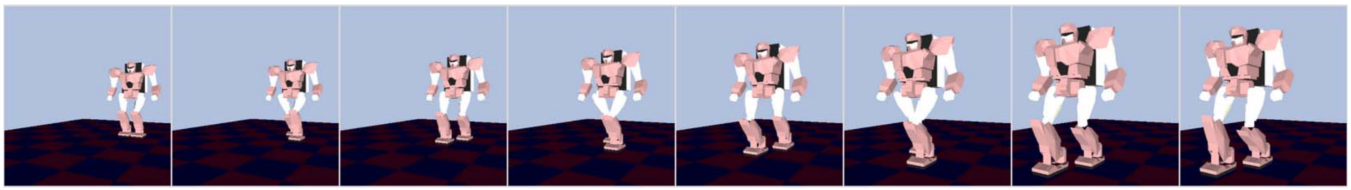

Fig. 13. Snapshots of a walking motion replayed by mighty.

References

[1] M. Vukobratović, A. A. Frank, and D. Juričić, "On the Stability of Biped Locomotion," *IEEE Transactions on Bio-Medical Engineering*, vol. BME-17, no. 1, pp. 25–36, 1970.

[2] J. Furusho and M. Masubuchi, "Control of a Dynamical Biped Locomotion System for Steady Walking," *Transactions of the ASME, Journal of Dynamic Systems, Measurement, and Control*, vol. 108, pp. 111–118, 1986.

[3] K. Mitobe, N. Mori, K. Aida and Y. Nasu, "Nonlinear feedback control of a biped walking robot," in *Proseedings of the 1995 IEEE International Conference on Robotics & Automation*, 1995, pp. 2865–2870.

[4] Y. Fujimoto, S. Obata, and A. Kawamura, "Robust Biped Walking with Active Interaction Control between Foot and Ground," in *Proceedings of the 1998 IEEE International Conference on Robotics & Automation*, 1998, pp. 2030–2035.

[5] D. C. Witt, "A Feasibility Study on Automatically-Controlled Powered Lower-Limb Prostheses," University of Oxford," Report, 1970.

[6] H. Miura and I. Shimoyama, "Dynamic Walk of a Biped," *The International Journal of Robotics Research*, vol. 3, no. 2, pp. 60–74, 1984.

[7] M. H. Raibert, H. B. B. Jr., and M. Chepponis, "Experiments in Balance with a 3D One-Legged Hopping Machine," *The International Journal of Robotics Research*, vol. 3, no. 2, pp. 75–92, 1984.

[8] S. Kajita and K. Tani, "Experimental Study of Biped Dynamic Walking in the Linear Inverted Pendulum Mode," in *Proceedings of the 1995 IEEE International Conference on Robotics & Automation*, 1995, pp. 2885–2819.

[9] M. Vukobratović and J. Stepanenko, "On the Stability of Anthropomorphic Systems," *Mathematical Biosciences*, vol. 15, no. 1, pp. 1–37, 1972.

[10] A. Takanishi, Y. Egusa, M. Tochizawa, T. Takeya, and I. Kato, "Realization of Dynamic Walking Stabilized with Trunk Motion," in *ROMANSY 7*, 1988, pp. 68–79.

[11] K. Hirai, M. Hirose, Y. Haikawa, and T. Takenaka, "The Development of Honda Humanoid Robot," in *Proceeding of the 1998 IEEE International Conference on Robotics & Automation*, 1998, pp. 1321–1326.

[12] K. Nagasaka, M. Inaba, and H. Inoue, "Walking Pattern Generation for a Humanoid Robot Based on Optimal Gradient Method," in *Proceedings of 1999 IEEE International Conference on Systems, Man, and Cybernetics*, 1999, pp. VI–908–913.

[13] Q. Huang, K. Yokoi, S. Kajita, K. Kaneko, H. Arai, N. Koyachi, and K. Tanie, "Planning Walking Patterns for a Biped Robot," *IEEE Transactions on Robotics and Automation*, vol. 17, no. 3, pp. 280–289, 2001.

[14] S. Kajita, F. Kanehiro, K. Kaneko, K. Fujiwara, K. Harada, K. Yokoi, and H. Hirukawa, "Biped Walking Pattern Generation by using Preview Control of Zero-Moment Point," in *Proceedings of the 2003 IEEE International Conference on Robotics & Automation*, 2003, pp. 1620–1626.

[15] K. Löffler, M. Gienger, and F. Pfeiffer, "Sensor and Control Design of a Dynamically Stable Biped Robot," in *Proceedings of the 2003 IEEE International Conference on Robotics & Automation*, 2003, pp. 484–490.

[16] K. Nagasaka, Y. Kuroki, S. Suzuki, Y. Itoh, and J. Yamaguchi, "Integrated Motion Control for Walking, Jumping and Running on a Small Bipedal Entertainment Robot," in *Proceedings of the 2004 IEEE International Conference on Robotics and Automation*, 2004, pp. 3189–3914.

[17] T. Sugihara and Y. Nakamura, "A Fast Online Gait Planning with Boundary Condition Relaxation for Humanoid Robots," in *Proceedings of the 2005 IEEE International Conference on Robotics & Automation*, 2005, pp. 306–311.

[18] T. Sugihara, Y. Nakamura, and H. Inoue, "Realtime Humanoid Motion Generation through ZMP Manipulation based on Inverted Pendulum Control," in *Proceedings of the 2002 IEEE International Conference on Robotics & Automation*, 2002, pp. 1404–1409.

[19] F. Gubina, H. Hemami, and R. B. McGhee, "On the dynamic stability of biped locomotion," *IEEE Transactions on Bio-Medical Engineering*, vol. BME-21, no. 2, pp. 102–108, 1974.

[20] S. Kajita, T. Yamaura, and A. Kobayashi, "Dynamic Walking Control of a Biped Robot Along a Potential Energy Conserving Orbit," *IEEE Transactions on Robotics and Automation*, vol. 8, no. 4, pp. 431–438, 1992.

[21] E. R. Westervelt, G. Buche, and J. W. Grizzle, "Experimental Validation of a Framework for the Design of Controllers that Induce Stable Walking in Planar Bipeds," *The International Journal of Robotics Research*, vol. 24, no. 6, pp. 559–582, 2004.

[22] T. McGeer, "Passive Dynamic Walking," *The International Journal of Robotics Research*, vol. 9, no. 2, pp. 62–82, 1990.

[23] M. Yamakita, F. Asano, and K. Furuta, "Passive Velocity Field Control of Biped Walking Robot," in *Proceedings of the 2000 IEEE International Conference on Robotics & Automation*, April 2000, pp. 3057–3062.

[24] S. H. Collins, M. Wisse, and A. Ruina, "A Three-Dimensional Passive-Dynamic Walking Robot with Two Legs and Knees," *The International Journal of Robotics Research*, vol. 20, no. 7, pp. 607–615, 2001.

[25] T. Sugihara, K. Yamamoto, and Y. Nakamura, "Hardware design of high performance miniature anthropomorphic robots," *Robotics and Autonomous System*, vol. 56, no. 1, pp. 82–94, 2007.